

Preparation, Characterization, and Kinetic Studies of Group 4 Metallocene Complexes with Triphenylsilylanetelluroate Ligands

David E. Gindelberger and John Arnold*

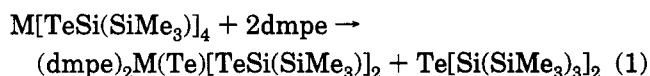
Department of Chemistry, University of California, Berkeley, California 94720

Received June 8, 1994[®]

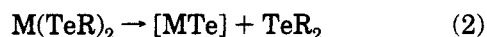
A range of new compounds incorporating the triphenylsilylanetelluroate ligand has been prepared and characterized. The required starting material was prepared by insertion of tellurium into the Li-Si bond of (THF)₃LiSiPh₃, which gave (THF)₃LiTeSiPh₃ in high yield. Protonolysis of (THF)₃LiTeSiPh₃ with trifluoroacetic acid resulted in the formation of the tellurol HTeSiPh₃ which is the first tellurol to be structurally characterized; it crystallized in the monoclinic space group *C2/c* with *a* = 16.208(3) Å, *b* = 11.343(3) Å, *c* = 19.979(3) Å, *β* = 114.45°, *Z* = 8, *R* = 0.0328, and *R_w* = 0.0409. The disilyl telluride Te(SiPh₃)₂ was prepared by reaction of (THF)₃LiTeSiPh₃ with Ph₃SiCl. The metallocene compounds (RCp)₂M(TeSiPh₃)₂ (M = Ti, R = H, Me (Cp⁺); M = Zr, R = H, Bu^t (Cp^t); M = Hf, R = H, Bu^t) were made by treatment of the appropriate metallocene dichloride with (THF)₃LiTeSiPh₃. Reaction of Cp^t₂Zr(TeSiPh₃)₂ with *tert*-butylpyridine gave clean elimination of Te(SiPh₃)₂ to form (Cp^t₂ZrTe)₂ as the only metal-containing product. Kinetic studies showed the reaction to be first-order in metallocene telluroate, implicating a mechanism involving intramolecular elimination of disilyl telluride. The X-ray structure of Cp^t₂Zr(TeSiPh₃)₂ is also described; it crystallized in the monoclinic space group *P2₁/n* with *a* = 9.460(1) Å, *b* = 26.177(2) Å, *c* = 16.442(1) Å, *β* = 96.79(1)°, *Z* = 4, *R* = 0.0277, and *R_w* = 0.0313.

Introduction

We recently initiated studies to probe the reactivity of early transition and lanthanide metal telluroate complexes in the expectation that single metal-chalcogen bonds comprising a hard, electropositive metal and a soft, polarizable chalcogen might exhibit some unusual and interesting chemistry.¹⁻⁵ In the case of the homoleptic Zr and Hf derivatives with the bulky -TeSi(SiMe₃)₃ ligand,³ addition of the chelating phosphine dmpe (dmpe = 1, 2-bis(dimethylphosphino)ethane) resulted in the elimination of disilyl telluride, as shown in eq 1; related reactions with tantalum were



also reported.⁴ These reactions are of interest for two reasons: (i) the metal complexes are rare examples of terminal tellurides,^{3,4,6-9} and (ii) these homogeneous, solution-state processes may be related to elimination reactions of the general type shown in eq 2, whereby metal telluroates are converted to solid-state metal tellurides.^{2,10-16}



In spite of recent advances, however, little is known regarding the mechanism of reactions of this type.^{17,18} Here we describe a number of interesting findings including the development of new telluroate synthons based on triphenylsilyl ligands, their use in preparing metallocene telluroate derivatives, and the first example of a crystallographically characterized tellurol. Kinetic data that shed light on the mechanism of a telluroate-to-telluride elimination reaction are also presented.

Results and Discussion

Triphenylsilylanetelluroate Synthons. Employing a reaction similar to that used to prepare [(THF)₃LiTeSi(SiMe₃)₃]₂,^{19,20} insertion of elemental tellurium into the

(11) Berardini, M.; Emge, T.; Brennan, J. G. *J. Am. Chem. Soc.* **1993**, *115*, 8501.

(12) Strzelecki, A. R.; Timinski, P. A.; Helsel, B. A.; Bianconi, P. A. *J. Am. Chem. Soc.* **1992**, *114*, 3159.

(13) Arnold, J.; Walker, J. M.; Yu, K. M.; Bonasia, P. J.; Seligson, A. L.; Bourret, E. D. *J. Cryst. Growth* **1992**, *124*, 647.

(14) Seligson, A. L.; Bonasia, P. J.; Arnold, J.; Yu, K.-M.; Walker, J. M.; Bourret, E. D. *Mater. Res. Soc. Symp. Proc.* **1992**, *282*, 665.

(15) Seligson, A. L.; Arnold, J. *J. Am. Chem. Soc.* **1993**, *115*, 8214.

(16) For leading references, see: (a) O'Brien, P. *Chemtronics* **1991**, *5*, 61. (b) Brennan, J. G.; Siegrist, T.; Carroll, P. J.; Stuczynski, S. M.; Reynders, P.; Brus, L. E.; Steigerwald, M. L. *Chem. Mater.* **1990**, *2*, 403. (c) Steigerwald, M. L.; Sprinkle, C. R. *J. Am. Chem. Soc.* **1987**, *109*, 7200. (d) Steigerwald, M. L.; Sprinkle, C. R. *Organometallics* **1988**, *7*, 245. (e) Bochmann, M.; Webb, K. J. *J. Chem. Soc., Dalton Trans.* **1991**, 2325. (f) Bochmann, M.; Webb, K. J.; Hursthouse, M. B.; Mazid, M. J. *Chem. Soc., Dalton Trans.* **1991**, 2317 and references in the above.

(17) Piers, W. E.; Macgillivray, L. R.; Zaworotko, M. *Organometallics* **1993**, *12*, 4723.

(18) Piers, W. E. *J. Chem. Soc., Chem. Commun.* **1994**, 309.

(19) Bonasia, P. J.; Gindelberger, D. E.; Dabboussi, B. O.; Arnold, J. *J. Am. Chem. Soc.* **1992**, *114*, 5209.

[®] Abstract published in *Advance ACS Abstracts*, October 1, 1994.

(1) Cary, D. R.; Arnold, J. *J. Am. Chem. Soc.* **1993**, *115*, 2520.

(2) Cary, D. R.; Arnold, J. *Inorg. Chem.* **1994**, *33*, 1791.

(3) Christou, V.; Arnold, J. *J. Am. Chem. Soc.* **1992**, *114*, 6240.

(4) Christou, V.; Arnold, J. *Angew. Chem., Int. Ed. Engl.* **1993**, *32*, 1450.

(5) Christou, V.; Wuller, S. P.; Arnold, J. *J. Am. Chem. Soc.* **1993**, *115*, 10545.

(6) Howard, W. A.; Parkin, G. *J. Am. Chem. Soc.* **1994**, *116*, 606.

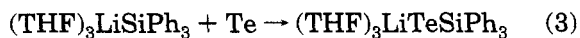
(7) Siemeling, U. *Angew. Chem., Int. Ed. Engl.* **1993**, *32*, 67.

(8) Rabinovich, D.; Parkin, G. *J. Am. Chem. Soc.* **1991**, *113*, 9421.

(9) Rabinovich, D.; Parkin, G. *J. Am. Chem. Soc.* **1993**, *115*, 9822.

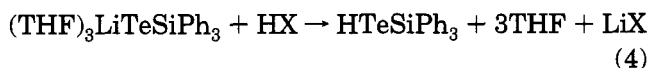
(10) Berardini, M.; Emge, T. J.; Brennan, J. G. *J. Chem. Soc., Chem. Commun.* **1993**, 1537.

Si-Li bond of $(\text{THF})_3\text{LiSiPh}_3$ afforded the silanetellurolate reagent $(\text{THF})_3\text{LiTeSiPh}_3$ as pale orange crystals in excellent yields (typically 80% on ca. 75 g scales) (eq 3). The tris-THF adduct is quite stable under an



atmosphere of dry nitrogen and does not lose solvent when exposed to vacuum for extended periods. Coordinated solvent is more labile in solution, however, with 1 equiv of THF being lost on recrystallization of the salt from toluene.

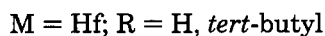
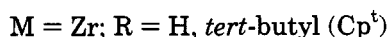
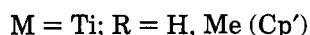
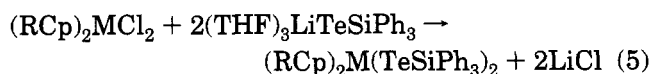
Protonation of a hexane suspension of $(\text{THF})_3\text{LiTeSiPh}_3$ affords the corresponding tellurol HTeSiPh_3 in reasonable yields (eq 4). If the acidification is carried out in more polar solvents, a partial decomposition occurs; for



example, when trifluoroacetic acid is added to an ether solution of $(\text{THF})_3\text{LiTeSiPh}_3$, the disilyl telluride $\text{Te}(\text{SiPh}_3)_2$ and H_2Te are generated in addition to the tellurol. A small amount of the latter compound was trapped at -196°C and characterized by ^1H NMR spectroscopy (-5.5 ppm²¹). Surprisingly, we have been unable to isolate the ditelluride $\text{Te}_2(\text{SiPh}_3)_2$, despite the fact that the related $-\text{Si}(\text{SiMe}_3)_3$ derivative is readily prepared by oxidation of the tellurolate anion with O_2 or CuCl and is extremely stable.²⁰ Reaction of the lithium salt with oxygen yields only $\text{Te}(\text{SiPh}_3)_2$ and other intractable products. Attempts to synthesize the ditelluride by reaction of the lithium tellurolate with cuprous chloride also gave the telluride and intractable solids.

Compared to compounds based on the $-\text{Si}(\text{SiMe}_3)_3$ ligand, those containing the $-\text{SiPh}_3$ group are much less soluble in hexane but dissolve well in other aromatic hydrocarbons and ethereal solvents. For example, HTeSiPh_3 is moderately soluble in hexanes (ca. 2 g/0.5 L), from which it crystallizes as large orange blocks, whereas $\text{HTeSi}(\text{SiMe}_3)_3$ is impossible to crystallize from this solvent due to its high solubility (ca. 1 g/mL). In addition, all of the SiPh_3 -based compounds are much more air sensitive than related $-\text{Si}(\text{SiMe}_3)_3$ or aryl derivatives. HTeSiPh_3 discolors slightly when left under nitrogen at room temperature for prolonged periods, and although the compound remains spectroscopically pure under these conditions, we recommend keeping it in a refrigerator at 0°C under nitrogen.

Synthesis and Characterization of Group 4 Metallocene Derivatives. Reaction of 2 equiv of $(\text{THF})_3\text{LiTeSiPh}_3$ with metallocene dichlorides affords the bis(tellurolate) derivatives in good yields (eq 5). This



reaction worked well for all of the metallocene derivatives except for $\text{Cp}^\dagger_2\text{TiCl}_2$, where only $\text{Te}(\text{SiPh}_3)_2$ was

Table 1. ^{125}Te Chemical Shifts for Selected Compounds

compd ^a	δ (ppm)	ref	compd	δ (ppm)	ref
$(\text{THF})_3\text{LiTeSiPh}_3$	-1337	a	$[(\text{THF})_2\text{LiTeSi}(\text{SiMe}_3)_2]$	-1622	b
$\text{Te}(\text{SiPh}_3)_2$	-851	a	$\text{Me}_2\text{SiTeSi}(\text{SiMe}_3)_3$	-1081	b
HTeSiPh_3	-684	a	$\text{HTeSi}(\text{SiMe}_3)_3$	-955	b
$[\text{Cp}^\dagger_2\text{ZrTe}]_2$	-130	a	$\text{Te}_2[\text{Si}(\text{SiMe}_3)_3]_2$	-678	b
$\text{Cp}_2\text{Ti}(\text{TeSiPh}_3)_2$	709	a	$\text{Cp}_2\text{Ti}[\text{TeSi}(\text{SiMe}_3)_3]_2$	810	c
$\text{Cp}^\dagger_2\text{Ti}(\text{TeSiPh}_3)_2$	659	a	$\text{Cp}^\dagger_2\text{Ti}[\text{TeSi}(\text{SiMe}_3)_3]_2$	783	c
$\text{Cp}_2\text{Zr}(\text{TeSiPh}_3)_2$	15	a	$\text{Cp}_2\text{Zr}[\text{TeSi}(\text{SiMe}_3)_3]_2$	-26	c
$\text{Cp}^\dagger_2\text{Zr}(\text{TeSiPh}_3)_2$	75	a			
$\text{Cp}_2\text{Hf}(\text{TeSiPh}_3)_2$	-170	a	$\text{Cp}_2\text{Hf}[\text{TeSi}(\text{SiMe}_3)_3]_2$	-233	c
$\text{Cp}^\dagger_2\text{Hf}(\text{TeSiPh}_3)_2$	-117	a			

^a This work. ^b Bonasia, P. J.; Gindelberger, D. E.; Dabboussi, B. O.; Arnold, J. *J. Am. Chem. Soc.* **1992**, *114*, 5209. ^c Christou, V.; Wuller, S. P.; Arnold, J. *J. Am. Chem. Soc.* **1993**, *115*, 10545.

isolated from the complex mixture of products. We have found that in many cases tellurolysis, using $\text{HTeSi}(\text{SiMe}_3)_3$ and a metal alkyl or amide, is preferable to metathesis due to the fact that it usually gives cleaner products and higher yields.^{2,3,22,23} In the present case, however, tellurolysis offers no particular advantage, as metathesis is simpler and gives roughly the same yields of pure products.

As expected, the compounds are less soluble in aliphatic hydrocarbons than the corresponding $-\text{TeSi}(\text{SiMe}_3)_3$ derivatives and are best crystallized from aromatic hydrocarbon or ethereal solvents. The bis(tellurolates) are highly colored with UV-vis spectra that are all slightly blue-shifted relative to their $-\text{TeSi}(\text{SiMe}_3)_3$ analogues. Tellurium-125 NMR data for all new compounds are collected in Table 1 along with analogous data for the corresponding $-\text{TeSi}(\text{SiMe}_3)_3$ derivatives for comparison. A wide range of chemical shifts is observed for the $-\text{TeSiPh}_3$ compounds, from -1337 ppm for the lithium salt to 709 ppm in the titanocene bis(tellurolate). These data are similar to those for materials containing the $-\text{TeSi}(\text{SiMe}_3)_3$ group,⁵ although note that here the range is slightly wider. Figure 1 shows a plot of the lowest energy visible absorption and ^{125}Te chemical shifts for both sets of compounds. It is well-known that for shielding of heavy nuclei, the paramagnetic term (σ^{para}) dominates the shielding equation and that this parameter is strongly influenced by low-level excited states,²⁴ such that

$$\sigma^{\text{para}} = \Delta E^{-1} \cdot \text{constant}$$

Thus, for a homologous series of compounds the paramagnetic term (which opposes σ^{diag} and is therefore deshielding) decreases linearly with increasing electronic excitation energy. In other words, compounds with low energy (visible) absorptions display low-field NMR shifts and vice versa.²⁵

Reactivity Studies. In our recent studies of the behavior of $\text{Cp}_2\text{M}[\text{TeSi}(\text{SiMe}_3)_3]_2$ complexes toward Lewis bases, we found that only the Ti derivative was reactive under the relatively mild conditions examined.⁵ As

(20) Bonasia, P. J.; Christou, V.; Arnold, J. *J. Am. Chem. Soc.* **1993**, *115*, 6777.

(21) Glidewell, C.; Rankin, D. W. H.; Sheldrick, G. M. *Trans. Faraday Soc.* **1969**, *65*, 1409.

(22) Gindelberger, D. E.; Arnold, J. *J. Am. Chem. Soc.* **1992**, *114*, 6242.

(23) Bonasia, P. J.; Arnold, J. *Inorg. Chem.* **1992**, *31*, 2508.

(24) Karplus, M.; Pople, J. A. *J. Chem. Phys.* **1963**, *38*, 2803.

(25) For a similar correlation in ^{13}C NMR spectroscopy, see: Breitmaier, E.; Voelter, W. *Carbon-13 NMR Spectroscopy*; VCH: New York, 1987, p 110.

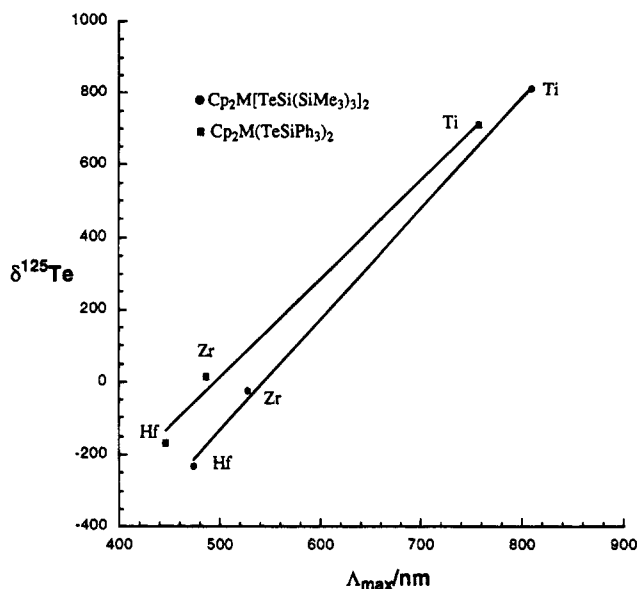
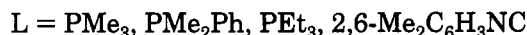
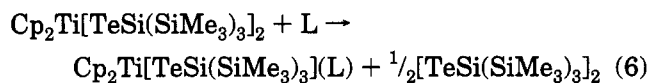


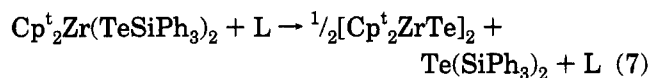
Figure 1. Plot of ^{125}Te NMR shift versus lowest energy electronic absorption for metallocene bis(tellurolates).

shown in eq 6, redox chemistry involving Ti(IV/III) is



the predominant pathway. For the $-\text{TeSiPh}_3$ derivatives, however, rather different modes of reactivity were observed. For both the Ti and Zr complexes, reactions with various Lewis bases in nonpolar solvents yielded insoluble metal-containing species and $\text{Te}(\text{SiPh}_3)_2$. The reactions were most complex for titanium, where dark mixtures were formed that made complete characterization impossible.

For zirconium, the corresponding reactions were much cleaner and more straightforward. $\text{Cp}_2\text{Zr}(\text{TeSiPh}_3)_2$ reacted with a variety of Lewis bases in toluene to form a dark red insoluble microcrystalline solid and $\text{Te}(\text{SiPh}_3)_2$. A parent peak at m/z 698 corresponds to the bridging telluride complex $[\text{Cp}_2\text{ZrTe}]_2$; however, the material could not be analyzed further, as it is insoluble in nonreactive solvents. This problem was solved by examining the reactivity of the Cp^t derivatives which, under similar conditions, yielded the soluble bridging telluride $[\text{Cp}^t_2\text{ZrTe}]_2$ and $\text{Te}(\text{SiPh}_3)_2$ (eq 7). The identity



of the zirconocene telluride complex was confirmed by comparison to literature data²⁶ and independent synthesis. Isolation of $\text{Te}(\text{SiPh}_3)_2$ from the reaction allowed it to be characterized by ^1H and ^{13}C NMR spectroscopy. The hafnium derivative reacts in an analogous fashion. No intermediates were observed spectroscopically and we found no evidence for incorporation of any Lewis base into the products.

The reaction shown above in eq 7 with $\text{L} = \text{tert}$ -butylpyridine was monitored by ^1H NMR spectroscopy

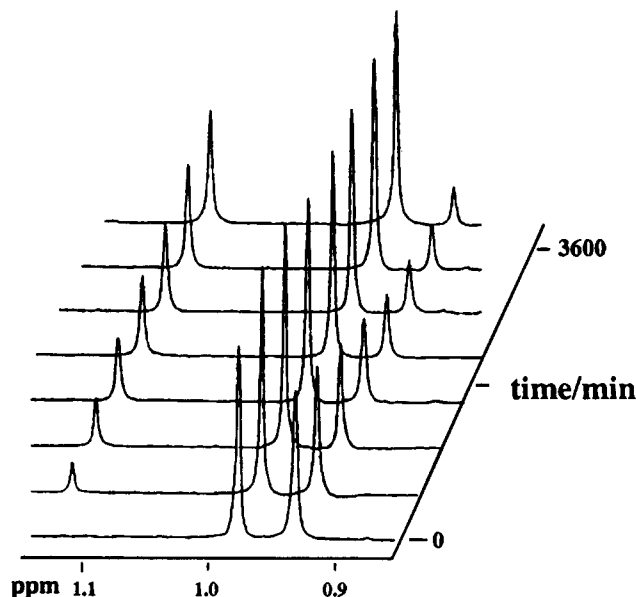


Figure 2. Portion of ^1H NMR spectrum for the reaction of $\text{Cp}^t_2\text{Zr}(\text{TeSiPh}_3)_2$ with *tert*-butylpyridine in toluene- d_8 at 90°C .

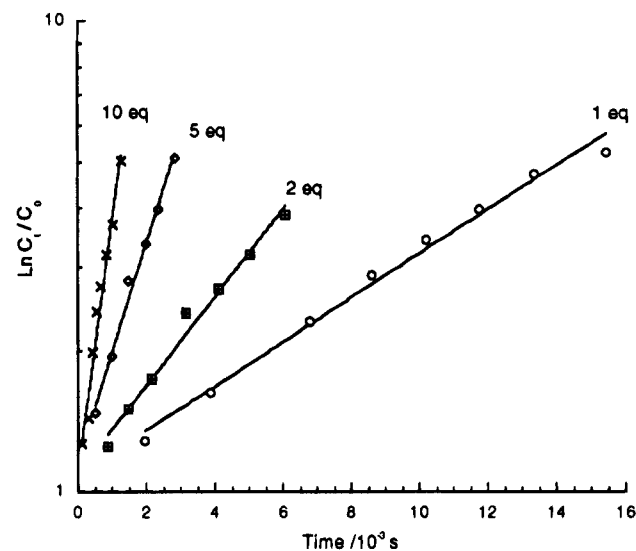
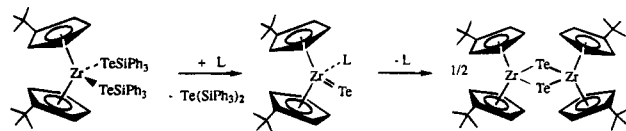


Figure 3. Plot of $\ln [(\text{Cp}_2\text{ZrTe})_2]$ versus time for the reaction of $\text{Cp}_2\text{Zr}(\text{TeSiPh}_3)_2$ with various concentrations of *tert*-butylpyridine in toluene- d_8 at 90°C .

in toluene- d_8 at 90°C . Figure 2 shows the *tert*-butyl region of the spectrum as the reaction proceeds. These data show that loss of starting material and appearance of product occur at the same first-order rate and that the reaction is catalytic in *tert*-butylpyridine (Figure 3). As seen in Figure 4, the rate is also linearly dependent on the concentration of added base. These data are consistent with a second-order reaction that is first-order in both the metal complex and base, as shown in the following scheme:



Moreover, our results show that elimination of $\text{Te}(\text{SiPh}_3)_2$ from the bis(tellurolate) is an *intramolecular* process. The putative terminal telluride intermediate

(26) Erker, G.; Nolte, R.; Tainturier, G.; Rheingold, A. *Organometallics* 1989, 8, 454.

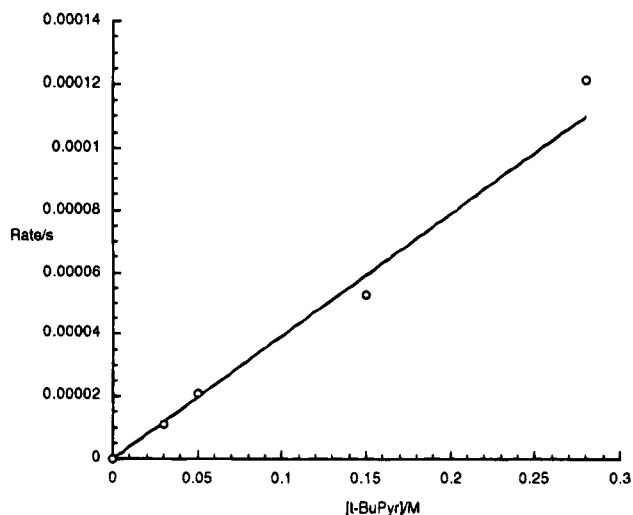


Figure 4. Plot of first order rate constant versus [*tert*-butylpyridine] for the reaction of $\text{Cp}^*_2\text{Zr}(\text{TeSiPh}_3)_2$ with various concentrations of *tert*-butylpyridine in toluene- d_8 at 90 °C.

was not observed; however, closely related Cp^* analogues were recently isolated and fully characterized.⁶ Evidently, loss of pyridine and dimerization of the terminal telluride species to form the bis(μ -telluride) complex is much more favorable when the Cp ligand is only monosubstituted. Attempts to prepare Cp^*_2Zr bis-(tellurolate) derivatives to test this hypothesis failed, presumably as a result of excessive steric demands.

This is the first mechanistic information to be reported for elimination of TeR_2 from a bis(tellurolate). Piers et al.¹⁸ recently reported mechanistic details for elimination of TeR_2 from $\text{Cp}^*_2\text{ScTeR}$ ($\text{R} = \text{CHDCHD-Bu}^t$); in this *mono*(tellurolate) system, the reaction proceeded with retention of the stereochemical probe, implying a concerted reaction via a bimolecular transition state. We are carrying out a more detailed kinetic analysis of our system, the results from which will be presented separately.²⁷

X-ray Crystallography. A summary of data collection parameters for all crystallographically characterized compounds is given in Table 2. The solid-state structure of HTeSiPh_3 is shown in Figure 5. The Te-Si bond length (Table 3) is similar to previously reported values, as are the Si-C distances and angles about the central silicon which are close to tetrahedral. The tellurolic hydrogen was not located despite collection of equivalent and high angle reflections. The corresponding triphenylsilanethiol²⁸ and triphenylsilyl alcohol²⁹ have been reported, and although the structures are related, there are significant differences in the degrees to which the monomeric units aggregate in the solid state. The silanol is tetrameric in the solid state ($\text{O-O} = 2.654 \text{ \AA}$), presumably as a result of hydrogen bonding, whereas the thiol and tellurol are monomeric. The tellurol has no close contacts between monomers, and the Te-Te distance ($4.6412(6) \text{ \AA}$) is outside the sum of van der Waals radii (4.40 \AA). A recent report of the structure of the first crystallographically characterized selenol ($2,4,6\text{-}(\text{CF}_3)_3\text{C}_6\text{H}_2\text{SeH}$) shows that this is also

Table 2. Summary of X-ray Diffraction Data

compd	HTeSiPh_3	$\text{Cp}_2\text{Zr}[\text{TeSiPh}_3]_2$
formula	$\text{C}_{18}\text{H}_{16}\text{SiTe}$	$\text{C}_{46}\text{H}_{40}\text{Si}_2\text{Te}_2\text{Zr}$
mol wt	388.01	955.41
T (°C)	-85	-91
space group	$C2/c$	$P2_1/n$
$a/\text{\AA}$	16.208(3)	9.460(1)
$b/\text{\AA}$	11.343(3)	26.177(2)
$c/\text{\AA}$	19.979(3)	16.442(1)
α/deg	90.0	90.0
β/deg	114.45(2)	96.79(1)
γ/deg	90.0	90.0
$\text{vol}/\text{\AA}^3$	3343(2)	4043(1)
Z	8	4
d_{calcd} (g cm^{-3})	1.541	1.635
cryst size/mm	$0.50 \times 0.40 \times 0.30$	$0.30 \times 0.25 \times 0.20$
scan mode	$\theta-2\theta$	Ω
2θ range/deg	3-55	3-45
collcn range	$+h, \pm k, \pm l$	$+h, +k, \pm l$
absn coeff, cm^{-1}	18.40	17.74
no. of unique reflns	3819	5803
no. of reflns with $F^2 > 3\sigma(F^2)$	2708	4319
final R, R_w	0.0328, 0.0409	0.0277, 0.0313

hydrogen bonded in the solid state.³⁰ Here, the selenol monomers are associated in a continuous zigzag pattern with an Se-Se contact 0.418 \AA less than the sum of van der Waals radii. Triphenylsilanols' limited ability to hydrogen bond demonstrates that steric effects do not prevent aggregation in triphenylsilanechalcogenols, and therefore, we ascribe the absence of hydrogen bonding in the tellurol to the small charge-to-radius ratio and low electronegativity of tellurium.

A view of the molecular structure of $\text{Cp}_2\text{Zr}(\text{TeSiPh}_3)_2$ is shown in Figure 6. As expected, the structure is quite similar to that of $\text{Cp}_2\text{Zr}[\text{TeSi}(\text{SiMe}_3)_3]_2$ reported recently.⁵ The Te-Zr angle (100.77° , see Table 4) is smaller than that found in the $-\text{TeSi}(\text{SiMe}_3)_3$ derivative (106.32°), due no doubt to differences in the steric bulk of the two silyl ligands. The Zr-Te distances (average 2.876 \AA) are close to those found in $\text{Cp}_2\text{Zr}[\text{TeSi}(\text{SiMe}_3)_3]_2$ (2.866 \AA), as is the Cp-Zr-Cp angle (130.5° vs 131.29°). For $\text{Cp}_2\text{Zr}(\text{TeSiPh}_3)_2$ two different Cp-Zr-Te angles are observed for each Cp ligand and seem to be a result of a steric interaction between the Cp ligands and the $-\text{SiPh}_3$ groups. When the molecule is viewed down a Zr-Te axis, the largest Cp-Zr-Te angle is between the Cp that is cis to the tellurium's silyl group. The Zr-Te-Si angles ($119.23, 116.56^\circ$) are more acute than found in $\text{Cp}_2\text{Zr}[\text{TeSi}(\text{SiMe}_3)_3]_2$ (123.32°), again due to differing steric demands of the substituents involved. The angles and distances about silicon are unexceptional.

Experimental Section

Unless noted otherwise all operations were carried out under a dry nitrogen atmosphere using a combination of glovebox and Schlenk-line techniques. Tetrahydrofuran, diethyl ether, toluene, and hexanes (all from Fisher) were predried over 4 \AA molecular sieves and distilled from sodium/benzophenone under N_2 . All NMR solvents were dried similarly but were distilled by vacuum transfer. Chlorotriphenylsilane (Hüls) and tellurium powder (Strem) were used as received. Trifluoroacetic acid (Aldrich) was degassed prior to use. The compounds $\text{Cp}^*_2\text{MCl}_2$ ($\text{M} = \text{Zr, Hf}$) were prepared

(27) Gindelberger, D. E. Work in progress.

(28) Minkwitz, R.; Kornath, A.; Preut, H. *Z. Anorg. Allg. Chem.* **1993**, *619*, 877.

(29) Puff, H.; Braun, K.; Reuter, H. *J. Organomet. Chem.* **1991**, *409*, 119.

(30) Labahn, D.; Bohnen, F. M.; Herbst-Irmer, R.; Pohl, E.; Stalke, D.; Roesky, H. W. *Z. Anorg. Allg. Chem.* **1994**, *620*, 41.

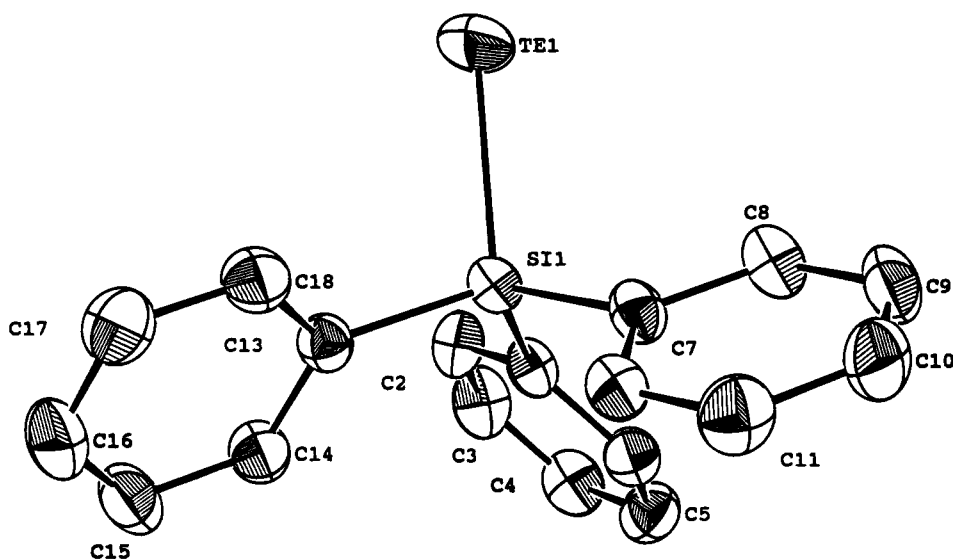


Figure 5. ORTEP view of the molecular structure of HTeSiPh₃.

Table 3. Selected Metrical Parameters for HTeSiPh₃

bond distances (Å)		bond angles (deg)	
Te—Si1	2.511(1)	Te1—Si1—C1	106.0(1)
Si1—C1	1.867(3)	Te1—Si1—C7	109.6(1)
Si1—C7	1.870(3)	Te1—Si1—C13	108.2(1)
Si1—C13	1.868(3)	C1—Si1—C7	111.8(1)
C—C _{av}	1.386	C1—Si1—C13	110.9(1)
Te—Te	4.6412(6)	C7—Si1—C13	110.3(1)

according to literature methods.³¹ Melting points were determined in sealed capillaries under nitrogen and are uncorrected. IR samples were prepared as Nujol mulls between KBr plates. Chemical shifts (δ) for ¹H NMR spectra are relative to residual protium in the deuterated solvents listed (e.g., C₆D₆, δ 7.15 ppm). Chemical shifts for ¹²⁵Te NMR spectra are relative to TeMe₂ at 0 ppm by reference to external Te(OH)₆ in D₂O (1.74 M) at δ 712 ppm and were performed at ambient temperatures in 5 mL tubes at 94.5726 MHz. Elemental analyses and EI/MS measurements were performed within the College of Chemistry, University of California, Berkeley.

(THF)₃LiTeSiPh₃. Li wire (6.9 g, 0.99 mol) was cut into small strips and placed into a flask containing Ph₃SiCl (36.4 g, 0.123 mol). The flask was cooled to -40 °C, and THF (375 mL) was added. The reaction mixture was allowed to warm slowly to room temperature and was stirred for 12 h. The mixture was then added to a cold (-40 °C) flask containing tellurium (15.8 g, 0.123 mol). The solution was again allowed to warm gradually and was stirred 12 h. The dark orange solution was filtered through a Celite pad, and the filtrate was evaporated under vacuum. The resulting oil was triturated with hexanes (2 × 100 mL) to give the product as pale orange microcrystals (61.3 g, 81%). Recrystallization from THF/hexanes (1:1) afforded analytically pure material, although the crude product was generally used in subsequent syntheses without noticeable deterioration in yield or purity. Mp: 224–227 °C. ¹H NMR (300 MHz, C₆D₆): δ 8.07 (d, 6 H, 6 Hz), 7.20 (m, 9 H), 3.49 (m, 12 H), 1.27 (m, 12 H). ¹³C{¹H} NMR (75.4 MHz, C₆D₆): δ 155.1, 136.9, 127.2, 125.0, 68.4, 25.4. ¹²⁵Te{¹H} NMR: δ -1337 (s, $\Delta\nu_{1/2}$ = 49 Hz). IR: 1426 (m), 1342 (w), 1329 (w), 1303 (w), 1293 (w), 1259 (w), 1183 (m), 1095 (s), 1075 (m), 1063 (m), 1046 (s), 919 (sh), 893 (s), 861 (sh), 742 (s), 702 (m), 879 (m), 598 (s) cm⁻¹. Anal. Calcd for C₃₀H₃₉O₃TeLiSi: C, 59.7; H, 6.52. Found: C, 59.5; H, 6.69.

HTeSiPh₃. Trifluoroacetic acid (0.5 mL, 7 mmol) was added dropwise to a slurry of (THF)₃LiTeSiPh₃ (4.0 g, 6.6 mmol) in hexanes. The mixture slowly turned light gray. After 30 min

of stirring, the mixture was filtered and the residue was extracted with hexanes (2 × 100 mL). The extracts were combined, and cooled to -40 °C. Two crops of orange crystalline product were collected (1.43 g, 57%). Mp: 151–153 °C. ¹H NMR (400 MHz, C₆D₆): δ 7.65 (d, 6 H, 7 Hz), 7.09 (m, 12 H), -6.45 (s, 1 H, J_{HTe} = 27.4 Hz). ¹³C{¹H} NMR (100 MHz, C₆D₆): δ 136.2, 134.8, 130.4, 128.4. ¹²⁵Te{¹H} NMR: δ -684 (s). ¹²⁶Te NMR: δ -684 (d, J_{TeH} = 27.4 Hz). IR: 2022 (w), 1427 (s), 1262 (m), 1107 (s), 1026 (m), 997 (m), 800 (m), 738 (m), 711 (m), 696 (s), 496 (s) cm⁻¹. EI/MS: m/z 389 (M⁺).

Te(SiPh₃)₂(CH₂Cl)_{0.25}. Toluene (30 mL) was added to a mixture of (THF)₃LiTeSiPh₃ (1.0 g, 1.6 mmol) and Ph₃SiCl (0.48g, 1.6 mmol). This solution was stirred for 20 h, and then the solvent was removed in vacuo. The residue was extracted with methylene chloride (50 mL) and filtered. The volume of the yellow filtrate was reduced to 20 mL, and the solution was cooled to -40 °C to yield a crop of colorless crystals (0.67 g, 61%). Mp: 229–230 °C. ¹H NMR (400 MHz, C₆D₆): δ 7.53 (d, 12 H, 7 Hz), 7.05 (t, 7 H, 6 Hz), 6.97 (t, 6 H, 7 Hz). ¹³C{¹H} NMR (75.4 MHz, C₆D₆): δ 136.5, 134.6, 129.9, 128.1. ¹²⁵Te{¹H} NMR: δ -851 (s, $\Delta\nu_{1/2}$ = 10 Hz). IR: 1426 (s), 1327 (w), 1304 (w), 1261 (w), 1180 (m), 1157 (w), 1106 (s), 1067 (m), 1025 (m), 998 (m), 740 (m), 709 (s), 696 (s), 677 (m) cm⁻¹. EI/MS: m/z 648 (M⁺). Anal. Calcd for C_{36.25}H_{30.5}Cl_{0.50}TeSi₂: C, 65.2; H, 4.60. Found: C, 65.3; H, 4.66.

Metalocene Derivatives. The procedure used to prepare all derivatives was essentially identical to that described in detail below for Ti.

Cp₂Ti(TeSiPh₃)₂. Toluene (100 mL) was added to a mixture of Cp₂TiCl₂ (0.97 g, 3.9 mmol) and (THF)₃LiTeSiPh₃ (5.0 g, 8.1 mmol) in a round-bottomed flask. The reaction mixture quickly turned black. The solution was stirred for 18 h, and the solvent was removed in vacuo. The resulting black residue was extracted with toluene (100, 50 mL) and filtered. After the filtrate was cooled to -40 °C, a crop of black crystalline solid was collected; two further crops gave a total yield of 2.8 g (75%) of pure product (mp 209–211 °C). ¹H NMR (300 MHz, C₆D₆): δ 8.04 (d, 12 H, 7 Hz), 7.21 (m, 18 H), 5.70 (s, 10 H). ¹²⁵Te{¹H} NMR: δ 709 (s, $\Delta\nu_{1/2}$ = 81 Hz). IR: 1425 (m), 1183 (w), 1155 (w), 1095 (m), 1025 (w), 1016 (w), 998 (w), 917 (w), 849 (w), 814 (m), 740 (m), 703 (s), 676 (m), 494 (s) cm⁻¹. Anal. Calcd for C₄₆H₄₀Si₂TiTe₂: C, 58.0; H, 4.23. Found: C, 58.3; H, 4.34. λ_{max} : 758 nm.

Cp₂Zr(TeSiPh₃)₂. Yield: red crystals, 71%. Mp: 180–186 °C dec. ¹H NMR (300 MHz, C₆D₆): δ 8.04 (d, 12 H, 7 Hz), 7.16 (m, 18 H), 5.61 (s, 10 H). ¹²⁵Te{¹H} NMR: δ 15 (s, $\Delta\nu_{1/2}$ = 48 Hz). IR: 1427 (m), 1306 (w), 1260 (w), 1184 (w), 1156 (w), 1103 (s), 1015 (w), 998 (w), 809 (w), 740 (m), 698 (s), 672

(31) Howie, R. A.; McQuillan, G. P.; Thompson, D. W.; Lock, G. A. *J. Organomet. Chem.* **1986**, *303*, 213.

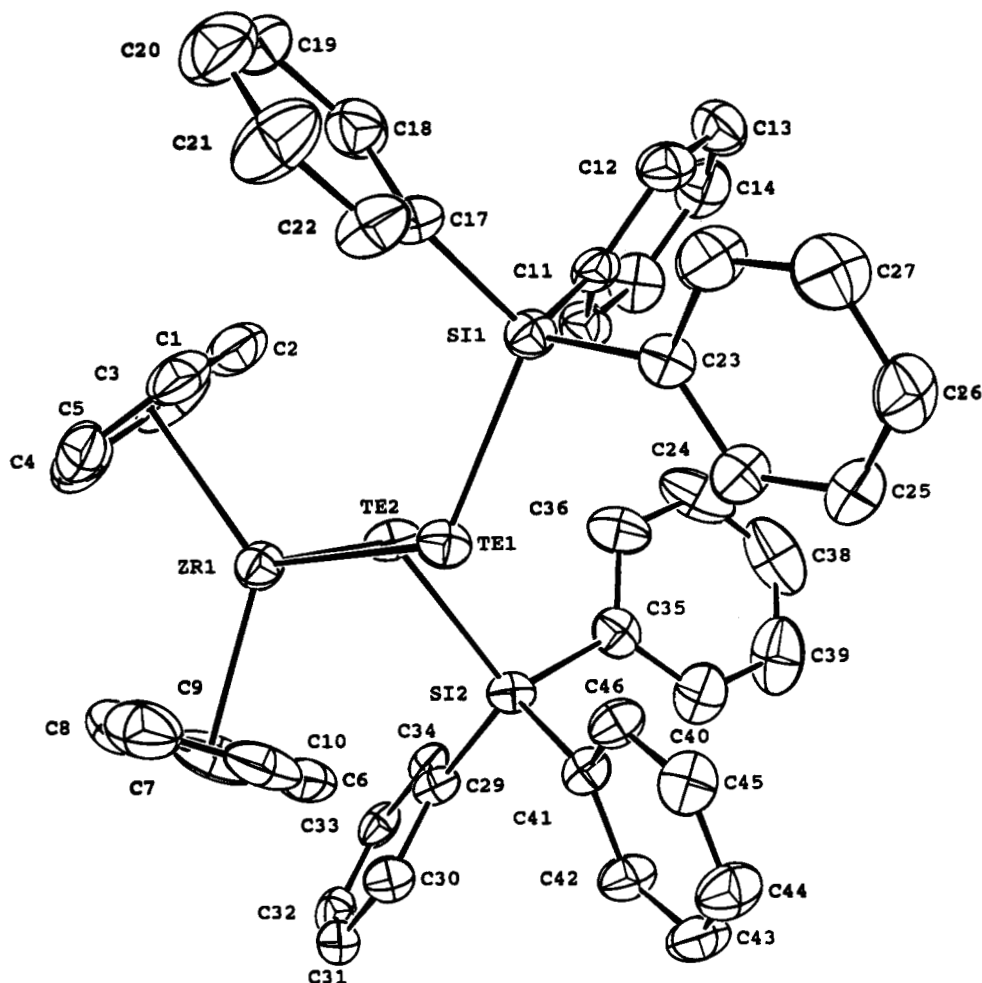


Figure 6. ORTEP view of the molecular structure of $\text{Cp}_2\text{Zr}(\text{TeSiPh}_3)_2$.

Table 4. Selected Metrical Parameters for $\text{Cp}_2\text{Zr}(\text{TeSiPh}_3)_2$

bond distances (Å)		bond angles (deg)	
Zr—Te1	2.8654(6)	Te1—Zr—Te2	100.77(2)
Zr—Te2	2.8873(7)	Cp—Zr—Cp	130.5
Zr—C _{av}	2.494	Cp1—Zr—Te1	109.2
Zr—Cp1 (centroid)	2.200	Cp1—Zr—Te2	102.2
Zr—Cp2 (centroid)	2.197	Cp2—Zr—Te1	100.9
Te1—Si1	2.485(1)	Cp2—Zr—Te2	109.7
Te2—Si2	2.498(1)	Zr—Te1—Si1	119.23(4)
Si—C _{av}	1.876	Zr—Te2—Si2	116.56(4)

(m) cm^{-1} . Anal. Calcd for $\text{C}_{46}\text{H}_{40}\text{Si}_2\text{Te}_2\text{Zr}$: C, 55.5; H, 4.05. Found: C, 55.2; H, 4.11. λ_{max} : 486 nm.

$\text{Cp}_2\text{Hf}(\text{TeSiPh}_3)_2$. Yield: 67% of an orange solid. ^1H NMR (300 MHz, C_6D_6): δ 8.05 (d, 12 H, 7 Hz), 7.19 (m, 18 H), 5.52 (s, 10 H). $^{125}\text{Te}\{^1\text{H}\}$ NMR: δ -170 (s, $\Delta\nu_{1/2}$ = 28 Hz). IR: 1426 (m), 1306 (w), 1260 (w), 1183 (w), 1155 (w), 1098 (s), 1016 (m), 998 (w), 846 (w), 819 (s), 812 (s), 739 (m), 697 (s), 676 (m), 494 (s) cm^{-1} . UV-vis (toluene): λ_{max} 446 nm.

$\text{Cp}_2\text{Ti}(\text{TeSiPh}_3)_2$. Yield: 55%. Mp: 206–210 °C. ^1H NMR (300 MHz, C_6D_6): δ 7.96 (d, 12 H, 6 Hz), 7.18 (m, 18 H), 5.95 (t, 4 H, 10 Hz), 5.80 (t, 4 H, 10 Hz), 1.45 (s, 6 H). $^{125}\text{Te}\{^1\text{H}\}$ NMR: δ 659 (s, $\Delta\nu_{1/2}$ = 66 Hz). IR: 1426 (m), 1257 (w), 1181 (w), 1098 (s), 894 (w), 811 (m), 739 (m), 701 (s), 676 (w), 493 (s) cm^{-1} . Anal. Calcd for $\text{C}_{46}\text{H}_{40}\text{Si}_2\text{TiTe}_2$: C, 58.8; H, 4.52. Found: C, 59.1; H, 4.38. λ_{max} : 752 nm.

$\text{Cp}_2\text{Zr}(\text{TeSiPh}_3)_2$. Yield: red crystals from toluene/hexane, 74%. Mp: 223–225 °C. ^1H NMR (300 MHz, C_6D_6): δ 8.09 (d, 12 H, 7 Hz), 7.23 (m, 18 H), 6.16 (t, 4 H, 3 Hz), 5.99 (t, 4 H, 3 Hz), 0.94 (s, 18 H). $^{125}\text{Te}\{^1\text{H}\}$ NMR: δ 75 (s, $\Delta\nu_{1/2}$ = 55 Hz). IR: 1481 (m), 1426 (s), 1366 (m), 1328 (w), 1304 (w), 1278 (m), 1189 (m), 1158 (m), 1101 (s), 1047 (m), 1027 (w), 998 (w), 913 (w), 870 (m), 819 (m), 802 (s), 743 (s), 696 (s), 676 (m), 494 (s)

cm^{-1} . Anal. Calcd for $\text{C}_{54}\text{H}_{56}\text{Si}_2\text{Te}_2\text{Zr}$: C, 58.5; H, 5.10. Found: C, 58.1; H, 5.38. λ_{max} : 526 nm.

$\text{Cp}^*_2\text{Hf}(\text{TeSiPh}_3)_2$. Yield: red-orange crystals from ether, 33%. Mp: 214 °C dec. ^1H NMR (300 MHz, C_6D_6): δ 8.11 (d, 12 H, 7 Hz), 7.23 (m, 18 H), 5.99 (t, 4 H, 3 Hz), 5.94 (t, 4 H, 3 Hz), 0.99 (s, 18 H). $^{125}\text{Te}\{^1\text{H}\}$ NMR: δ -117 (s, $\Delta\nu_{1/2}$ = 66 Hz). IR: 1426 (s), 1364 (m), 1279 (w), 1189 (w), 1159 (m), 1101 (s), 874 (m), 824 (m), 806 (s), 744 (m), 697 (s), 676 (w), 495 (s) cm^{-1} . λ_{max} : 474 nm.

$(\text{Cp}^*_2\text{ZrTe})_2$. A solution of $\text{Cp}^*_2\text{ZrCl}_2$ (0.50 g, 1.2 mmol) in 50 mL of THF was cooled to -78 °C. A solution of BuLi (1.1 mL, 2.2 M) was added using a syringe and the solution was stirred 30 min. Tellurium (0.16 g, 1.2 mmol) was added, and the solution was allowed to warm to room temperature at which time the mixture was deep red-violet. The solution was stirred an additional hour, and the solvent was removed in vacuo. The resulting red residue was extracted with toluene (30 mL), the volume was reduced to 10 mL, and the solution was cooled to -40 °C. Two crops of red crystals were collected by filtration (0.32 g, 58%). Mp: 329 °C dec (lit. 328 °C). ^1H data were identical to literature values.²⁶ $^{125}\text{Te}\{^1\text{H}\}$ NMR: δ -130 (s, $\Delta\nu_{1/2}$ = 55 Hz). IR: 1484 (m), 1357 (m), 1274 (m), 1201 (w), 1157 (m), 1041 (w), 1021 (w), 916 (w), 892 (w), 859 (m), 797 (s), 728 (w), 457 (w) cm^{-1} . λ_{max} : 574 nm.

$[\text{Cp}^*_2\text{HfTe}]_2$. THF (50 mL) was added to a mixture of $\text{Cp}^*_2\text{HfCl}_2$ (0.50 g, 1.0 mmol) and $\text{Na}_2\text{Te}^{32}$ (0.50 g, 2.9 mmol). The mixture was heated to reflux for 2 days, and the solvent was removed in vacuo. The solids were extracted with toluene and the solution was filtered through a fine frit. The solvent was again removed and the product was obtained by washing the solid with hexanes (2 × 25 mL). Yield: 0.12 g (22%). ^1H NMR

(300 MHz, C_6D_6): δ 6.71 (t, 4 H, 3 Hz), 6.63 (t, 4 H, 3 Hz), 1.21 (s, 18 H). IR: 1484 (m), 1362 (m), 1265 (m), 1262 (w), 1202 (w), 1158 (m), 1090 (w), 1042 (m), 1023 (w), 917 (w), 896 (w), 865 (w), 800 (s), 728 (w), 671 (w), 659 (w) cm^{-1} . UV-vis (toluene): λ_{max} : 518 nm.

Kinetics Experiments. The required amount of 4-*tert*-butylpyridine (ca. 1, 2, 5, or 10 equiv) was added to 1.00 mL of a 0.027 M toluene- d_8 solution of $Cp^*_2Zr(TeSiPh_3)_2$. The solution was divided into two equal portions and placed into Teflon-stoppered NMR tubes. The ratio of base/metallocene was then confirmed by 1H NMR spectroscopy. The tubes were heated at a constant temperature, either in the probe of the spectrometer or in a constant temperature bath, for the duration of the experiment. During the experiments a gradual color change from violet to red occurred. The rate of reaction was determined by following changes in peak area of the *tert*-butyl region, using the area of the *tert*-butyl group of 4-*tert*-butylpyridine as an internal standard.

X-ray Crystallography. Our standard operating procedures were followed.²³ The crystal structures were solved by Patterson methods. The data were then refined via standard least-squares and Fourier techniques. Table 2 contains details of the crystal data collection parameters.

HTeSiPh₃. Large clear orange cubes were obtained by cooling a saturated hexane solution to -40 °C. An appropriate crystal was selected ($0.50 \times 0.40 \times 0.30$ mm) and mounted on a quartz capillary under Paratone-N oil. The crystal was transferred to the diffractometer, centered in the beam, and cooled to -85 °C. Automatic peak search and indexing procedures yielded the possibility of a triclinic or C-centered monoclinic cell. The data were collected for the triclinic cell. Refinement in the triclinic system was unsatisfactory, and the data were converted to the monoclinic system. Inspection of

the systematic absences indicated the space group $C2/c$. The duplicate data was averaged and refinement continued satisfactorily. Hydrogen atoms were assigned idealized locations and were included in structure factor calculations, but were not refined. The final residuals for 242 variables refined against 2708 data for which $F^2 > 3\sigma(F^2)$ were $R = 0.0328$, $R_w = 0.0409$, and $GOF = 1.49$.

$Cp^*_2Zr(TeSiPh_3)_2$. Large red needles of the compound were obtained by slow diffusion of hexanes into a concentrated toluene solution. The crystal was mounted in a fashion similar to that described above and cooled to -91 °C. Automatic peak search and indexing procedures yielded a monoclinic reduced primitive cell. Inspection of the systematic absences indicated the space group $P2_1/n$. Hydrogen atoms were assigned idealized locations and were included in structure factor calculations, but were not refined. The final residuals for 460 variables refined against 4030 data for which $F^2 > 3\sigma(F^2)$ were $R = 0.0277$, $R_w = 0.0313$, and $GOF = 1.27$.

Acknowledgment. We are grateful to the National Science Foundation (Grant No. CHE-9210406) for financial support, to Dow Chemical for the award of a graduate fellowship to D.E.G., and to the Alfred P. Sloan Foundation for the award of a research fellowship to J.A.

Supplementary Material Available: Tables of positional parameters, intramolecular distances and angles, least-squares planes, and anisotropic thermal parameters for all structures (18 pages). Ordering information is given on any current masthead page.

OM940435T